Analysis of a Topology Control Paradigm in WLAN/WPAN Environments

A. Vaios

National & Kapodistrian University of Athens, Department of Informatics & Telecommunications

K. Oikonomou

National & Kapodistrian University of Athens, Department of Informatics & Telecommunications

I. Stavrakakis

National & Kapodistrian University of Athens, Department of Informatics & Telecommunications

Abstract

The coordinated coexistence of WLANs and WPANs in a *dual-mode* network is a recently introduced idea and is expected to increase the overall *system performance* by allowing for the efficient cooperation of both WLANs and WPANs. *Topology control* (e.g., power control, smart antennas, different frequency channels) needs to be employed to allow for the simultaneous operation of both modes. In this paper, different frequency channels that allow for *high data rates* within a *small transmission range* are considered in order to create multiple WPAN environments inside a WLAN cell. The latter environment requires the support of a second mode of operation which introduces additional *overhead* that may degrade the overall system performance. Certain conditions, under which system performance improvement is achievable, are established here. In particular, an analytical *mobility model* for WPAN environments is proposed and employed in the analytical studies. It is shown that the system may be effective when node *mobility* is low and the *traffic load* among nodes is high. The corresponding *upper* and *lower* bounds on mobility and traffic are also analytically derived. Simulation results for a variety of scenarios support the claims and expectations of the aforementioned analysis and demonstrate that performance improvement is possible when WLANs and WPANs coexist and cooperate in a network.

Key words: Mobility Model, WLAN, WPAN, Topology Control

1 Introduction

The evolving *third generation* (3G) of telecommunication systems focuses on the individual users and their needs for increased data rates. However, with the advance of the Wireless Local Area Network (WLAN) technologies in the last years, the adoption of WLANs as last mile networks in 3G systems has started to gain ground, (1), (2). As the demand for higher data rates increases due to the modern sophisticated applications, the central coordinator of a WLAN network (e.g., the Access Point depicted in Figure 1.a) becomes the obvious bottleneck node even when mobile terminals (MTs) that need to exchange large amounts of data between each other are located in the same cell (coverage area of the Access Point).

The idea of using a *second mode of operation*, has been recognized as a promising technique in order to increase the capacity of a WLAN network ((3) - (10)). In (9) and (10), the second mode of operation is employed in a different frequency, compared to the traditional WLAN one, allowing users, that want to exchange data locally, to operate in the network by applying high-rate, short-range communications and, at the same time, limit the *interference* imposed by the presence of other nodes in the WLAN cell. Figure 1.b depicts the case where MT A and MT B have switched to the second mode of operation in order to exchange data locally.

a.   First Mode of Operation.   b.   Support of a Second Mode of Operation.
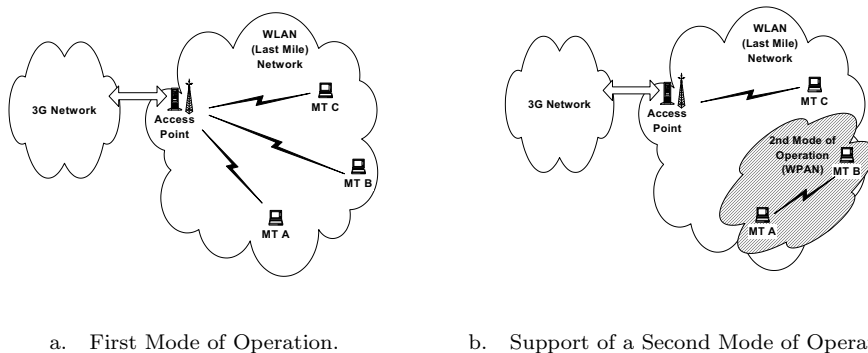
Fig. 1. Last mile network example. The Access Point of the WLAN is connected to the core 3G network.

The coexistence of two modes of operation along with the two distinct types of network topologies (the large WLAN umbrella containing potentially several WPAN islands which are called *clusters*) requires the application of some type of *topology control*. In this paper, topology control may be defined as a node's capability of controlling the set of its neighbor nodes, (11). A node u is a neighbor node to another node v, if a direct transmission from node

Email addresses: avaios@di.uoa.gr (A. Vaios), okon@di.uoa.gr (K. Oikonomou), ioannis@di.uoa.gr (I. Stavrakakis).

2

u to node v is possible. Power control and/or smart antennas may be used for topology control, ((12) - (20)). Power control can be applied to adapt the transmission power in accordance with the location of the receiver. Smart antennas may be employed in order for the nodes to be capable of adjusting transmission/reception angles. A third approach is to allow nodes to operate at different frequency channels, (9).

Under any of the aforementioned approaches, the coordination of the second mode of operation within the WLAN framework is challenging. The performance of the resulting system depends on various factors such as: (a) the mobility of the nodes; (b) the load of the data traffic; (c) the availability of the bandwidth, (9), (11). This work focuses on the first two factors assuming that the bandwidth provided by the second mode of operation is high compared to that under the customary first mode of operation (WLAN operation), as it is also discussed in Section 2. The design specification for the support of the second mode of operation using different frequency channels, presented in (10), is adopted here but it may be extended for any other approach used for topology control (smart antennas or power control). Under this specification, a second mode is established that supports high data rates for nodes close to each other that do not necessarily operate at the same frequency channel.

An essential component of the system design, presented in Section 2, is the *Neighborhood Discovery phase* (ND phase) that determines the set of neighbor nodes – with respect to the second mode of operation – of each node in the network. During the ND phase, all nodes are required to broadcast "hello" messages and consequently, additional *overhead* is introduced in the system. Two key modules, the *Neighborhood Discovery Indicator* (NDI) module and the *Centralized Clustering-Routing* (CCR) module, are responsible for determining the *time period* between two consecutive ND phases and the *set of nodes* that will operate in the second mode forming clusters, respectively. An analytically tractable model, capturing effectively the mobility behavior of the nodes inside a WPAN environment and taking also into consideration the wireless channel, is derived and studied in Section 3. This model is innovative and fairly realistic for personal area environments where users are expected to move close to the nodes that they want to communicate with. Analytical results leading to the derivation of the time period between consecutive ND phases that may be proved beneficial for the system are presented in Section 4. In Section 5, the overhead introduced for the support of the second mode of operation is considered in order to determine the conditions under which nodes creating clusters benefit from the second mode of operation. It is shown that the considered second mode of operation may be efficiently incorporated into the resulting system under certain mobility and traffic conditions, which are established in this work. Simulation results, presented in Section 6, support the claims and the expectations of the aforementioned analysis. The conclusions are drawn in Section 7.

The major contribution of this work is twofold: on the one hand, a novel mobility model that takes into account the wireless channel for the WPAN environment is introduced, while, on the other, performance aspects of the dual-mode system are analytically studied and validated through simulations. It should be noted that the basis of our analysis is the system described in (9) and (10), the key aspects of which are discussed in Section 2.

2 System Description

The design requirements for supporting a second mode of operation in a WLAN network using different frequency channels, were first presented in (9). The described system was based on HiperLAN/2, (21), but it could be easily extended for other WLAN systems (e.g., IEEE 802.11). According to the HiperLAN/2 standard, the Access Point (AP) is responsible for all operations in its 5 GHz cell. A second mode of operation at 60 GHz is possible, if certain new modules, described later in this section, are included in the standard HiperLAN/2 protocol stack, (10). Different frequency channels are available that allow nodes in close proximity to each other to operate without interfering with other nodes operating in the second mode of operation at different frequency channels and thus, achieving spatial reuse. The architecture, proposed in (9), may be viewed as a first step toward a new platform that would provide for an integrated WLAN/WPAN technology capable of meeting user expectations in terms of throughput and sophisticated application support.

There are some peculiarities regarding the 60 GHz mode of operation. On the one hand, high data rates are possible (over 100 Mbps as opposed to 54 Mbps under the standard mode of operation at 5 GHz) but, on the other, the range of transmission is reduced (10 meters or less as opposed to 50 meters), (9). Moreover, a link may exist only under line of sight (LOS) conditions.

The AP is possible to operate simultaneously at both frequency bands (5 and 60 GHz). This requires two *Radio Frequency* (RF) front-ends for the simultaneous operation of the AP at both frequency bands and, thus, modes. To keep the cost of a MT low though, each MT is equipped with one RF front-end, thus enabling only one mode of operation at a time and requiring for a mechanism for *switching* between the two modes of operation.

When MTs that need to exchange data are in proximity to each other, they create a cluster of MTs at 60 GHz and exchange data for a number of *frames*, as described in (9), (10) (each frame lasts for 2 ms). A certain node within each cluster, called the *clusterhead* (CH), is responsible for all operations inside a cluster, in a similar manner that the AP is responsible for all operations in its

cell at 5 GHz. The AP is assumed to be the CH of its corresponding cluster.

Communication between MTs in the same cluster (*intracluster* communication) is coordinated through the CH. Communication between nodes that belong to different clusters (*intercluster* communication) is also possible, provided that certain nodes assume the role of the *forwarding node* (FN), which has to switch between different frequency channels at 60 GHz. Examples of intracluster and intercluster communication at 60 GHz, and standard communication at 5 GHz, are depicted in Figure 2. This work is primarily focused on intracluster communication (that is possible by applying – and is also referred to as – the *second mode* of operation) as opposed to the standard communication at 5 GHz (also referred to as the *first mode* of operation).
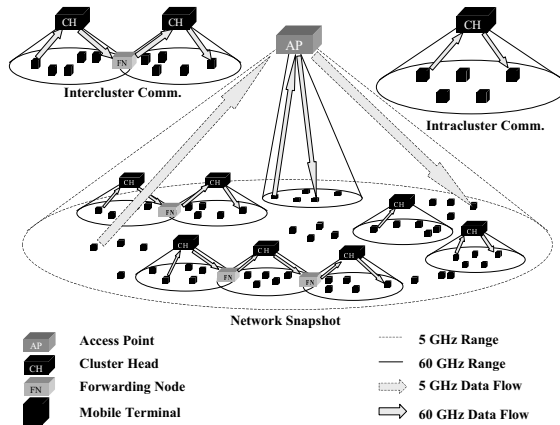

Fig. 2. Examples of intracluster and intercluster communication at 60 GHz, and standard communication at 5 GHz.

The dual mode of operation is supported by introducing additional functionality, as it is depicted in Figure 3. First of all, the set of neighbor nodes of each terminal at 60 GHz is determined. The ND phase is responsible for determining this set of nodes. This is realized by allowing for all nodes to switch at a particular frequency channel at 60 GHz and start exchanging "hello" messages. When the exchange of these messages is completed, each node is aware of its neighbors. Then, this *topological information* is forwarded to the AP which then becomes aware of the set of neighbor nodes at 60 GHz for all nodes in the network. Let f_{ND} denote the number of frames required for the completion of a ND phase. A summary of all parameters defined in this paper are included in Appendix C.

After the ND phase, which the *Neighborhood Discovery* (ND) module is responsible for, the topological information that is provided to the AP, along with the *resource demand information*, is used for the creation of the clusters. The resource demand information is available to the AP, since the AP is responsible for all operations and consequently, for the allocation of the resources at both the 5 GHz and the 60 GHz bands. The *Centralized Clustering-Routing*

5

(CCR) module is responsible for creating the clusters (*clustering information*) and the corresponding *routing information*.
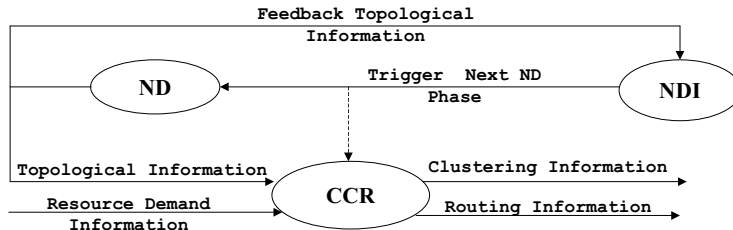

Fig. 3. Information flow among different modules.

Clusters are created dynamically by the AP based on topological and resource demand information and they are re-organized when this information changes and the AP is properly notified. The resource demand information is readily available to each node and is directly communicated to the AP (by each node). This is not the case with the (60 GHz) topological information which requires the execution of the ND phase to determine the current 60 GHz neighbors of each node.

The *Neighborhood Discovery Indicator* (NDI) module, depicted in Figure 3 is responsible for *triggering* the next ND phase. Let f_{NDI} denote the number of frames between two consecutive ND phases. Clearly, the higher the mobility of the nodes (or the number of link breakages), the more frequent the ND phases need to take place in order to provide more credible information about the 60 GHz links and consequently, the smaller the value of f_{NDI}. The NDI module specifies the value of f_{NDI} based on *feedback topological information*. For example, the NDI module may compare the new topological information with the previous one and infer – based on the rate of link changes – the current mobility conditions in the network.

From the above discussion, it is evident that all three modules (ND, NDI and CCR) are important for the operation of the dual mode system and they can strongly affect its effectiveness. Although they take critical decisions based on the provided information, these modules introduce significant *overhead* into the system operation. Frequent ND phases (small values for the f_{NDI}) introduce a significant amount of overhead due to the frequent consumption of the f_{ND} frames required for the completion of the ND phase. On the other hand, rare ND phases (large values for f_{NDI}) may lead to outdated and inaccurate clusters, not taking advantage of the extra bandwidth that the second mode of operation offers.

Since node mobility introduces changes in the topology, which should be taken into consideration in the design and operation of the system, it is important that an effective, analytically tractable model for capturing this mobility be developed and the main performance aspects be evaluated, to determine the

involved trade-offs and effectively set the system parameters.

3   The Mobility Model for WPAN Environments

In personal area environments, nodes are not moving randomly but tend to get closer to nodes that want to exchange data with. Therefore, a mobility model that is based on random node movement (e.g., the random waypoint model, (22)) may not be realistic. It is reasonable to assume that it is more likely than not that two nodes that are actually exchanging data to be close to each other (e.g., Bluetooth, conference rooms). It is also reasonable to assume that in the near future and as long as they continue to exchange data, these nodes will stay in the proximity of each other. After a certain time, these nodes will cease communicating either because at least one of them moves away or simply because of lack of connectivity for some other reason. In the sequel, a 2-state link status evolution model (Gilbert model) is introduced that inherently captures the aforementioned mobility behavior [1] and the resulting correlations in the link state. This model also accounts for link breakages due to the degradation of the wireless channel itself. In WPAN short-range environments, link failures are strongly affected by the propagation characteristics of the frequency band used.

For the remainder of this paper, a generic link in the second mode of operation between two nodes u and v will be considered. This link can be in one of two states: present (alive) or absent. Given that the link is present (absent) in the current frame, the probability that it is present (absent) in the next frame is fixed and equal to p (p'). That is, the state evolution of the link is modeled in terms of a 2-state Markov chain with transition probabilities p and p', as depicted in Figure 4. Based on this model, it is clear that the length of a period of continuous presence (absence) is geometrically distributed with parameter p (p').

Let J represent the number of frames that have elapsed since the creation of a cluster, assumed to have taken place at time frame $J = 0$. Let p_j be the

---

[1] Notice that the Gilbert (2-state Markov) model has been widely adopted for modeling the state of a link (good-bad) as shaped by the quality of the wireless communication channel (mostly static environment). Since in a typical mobile ad-hoc networking environment the state of the link is shaped primarily by the assumed random user mobility and secondarily by the wireless channel quality, a Gilbert model would not be appropriate for capturing the combined impact of mobility and channel quality. By relaxing the random mobility assumption in WPANs – as articulated above – and justifying the correlations in the mobility patterns of the nodes, the combined effect of mobility and channel quality can realistically now be modeled in terms of the Gilbert model.
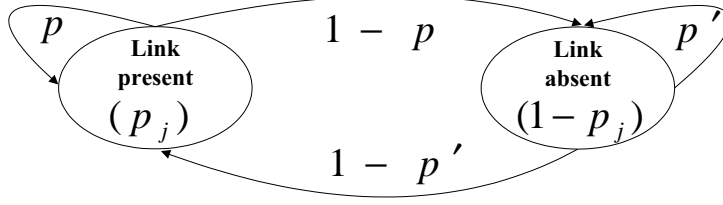
Fig. 4. Markov State Diagram.

conditional probability that link (u, v) is present at frame $J = j$ provided that it was present at frame $J = 0$, when the last ND phase was completed. Clearly, p_j corresponds to a j-step transition probability of the associated Markov chain (the analysis is included in Appendix A for completeness). It is given by

$$p_j = 1 - (1-p)\frac{1 - (-(1-p'-p))^j}{2-p-p'}. \tag{1}$$

The long term (steady-state) probability that the link is present is trivially obtained from the equilibrium equations of the 2-state Markov chain and it is given by $(j \rightarrow +\infty)$,

$$p_{+\infty} = \frac{1-p'}{2-p-p'}. \tag{2}$$

4   Repetition Frequency of the ND Phases

The aim of this section is to derive an analytical expression for an upper bound on f_{NDI} so that the number of links that break between two consecutive ND phase executions be bounded. This quantity will be directly linked to the mean number of frames between two consecutive ND phases, which will not be possible to utilize due to broken links, and finally to the wasted system capacity and the effectiveness of the dual-mode system. These derivations will assume both p and p' are known.

According to the markovian link state model introduced earlier, a certain link (u, v) that existed in frame $J = 0$, may not be present during the entire lifetime of a cluster (until a new ND phase takes place). Let the (average) number of frames that link (u, v) is present be denoted by $\overline{J}$, where $\overline{J} = \sum_{j=1}^{f_{NDI}} p_j$. According to Appendix B,

$$\overline{J} = f_{NDI} - (1-p)\frac{f_{NDI} + (1-p'-p)\frac{1-\left(-(1-p'-p)\right)^{f_{NDI}}}{2-p'-p}}{2-p'-p}. \qquad (3)$$

Let L_{NDI} denote the average number of frames over the time horizon between two consecutive ND phases (of total length of f_{NDI} frames), during which link (u, v) is absent and thus it cannot be used by the nodes u and v. $L_{NDI} = f_{NDI} - \overline{J}$ and according to Equation (3),

$$L_{NDI} = (1-p)\frac{f_{NDI} + (1-p'-p)\frac{1-\left(-(1-p'-p)\right)^{f_{NDI}}}{2-p'-p}}{2-p'-p}. $$

$$(4)$$

Clearly, the closer $\overline{J}$ to f_{NDI}, the more effective the operation of the NDI module ($L_{NDI} \to 0$).

Figure 5 depicts $\frac{L_{NDI}}{f_{NDI}}$ as a function of f_{NDI} for different values of p (0.1, 0.3, 0.7, 0.9). It may be seen that as f_{NDI} increases, $\frac{L_{NDI}}{f_{NDI}}$ converges to $p_{+\infty}$, irrespectively of the value of p ($p_{+\infty} = 0.5$ for $p' = p$). It can be seen that for large values of p (0.7 and 0.9), $\frac{L_{NDI}}{f_{NDI}}$ is very small for small values of f_{NDI}. This is expected since for large values of p, link (u, v) is likely to exist during the first frames after the activation of the cluster. However, after a certain number of frames, link (u, v) may not be present as the number of frames increases and the probability that link (u, v) is present at a frame $j \to +\infty$ converges to a certain value, $p_{+\infty}$, as it may also be concluded from Equation (2).
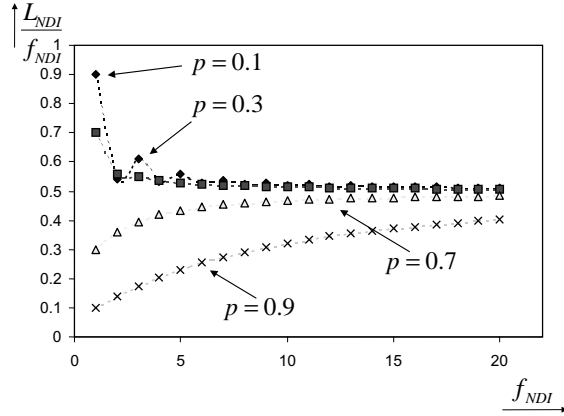

Fig. 5. $\frac{L_{NDI}}{f_{NDI}}$ as a function of f_{NDI} for different values of p (0.1, 0.3, 0.7, 0.9) and $p' = p$.

From the previous discussion it is evident that the smaller the value of f_{NDI}, the smaller the resulting value of L_{NDI}. However, due to the fact that the ND phase consumes a certain number of frames, f_{ND}, which are clearly an

9

overhead, small values for f_{NDI} may not be efficient for the system. On the other hand, since a large value of f_{NDI} would result in a high number of link failures, it would be useful to determine an upper bound on f_{NDI} so that the probability that a link failure takes place for the first time during a certain number of frames is bounded. It would be highly desirable for activated clusters not to fail until the next ND phase.

Let m_j denote the probability that link (u, v) fails for the first time at time frame $J = j$ (that is j frames after the last ND phase completion). Given that in frame $J = 0$ link (u, v) did exist, m_j is given by the following equation

$$m_j = (1 - p)p^{j-1}. \tag{5}$$

It is clear that as j increases, m_j decreases exponentially. On the other hand, as it may be observed from Figure 6, as p increases, m_j increases until the maximum is assumed, for a certain value of p (the maximum is assumed for that value of p, for which $\frac{dm_j}{dp} = 0$, or $p = \frac{j}{1+j}$, since the first derivative of m_j with respect to p is $\frac{dm_j}{dp} = (-p + (1 - p)j)p^{j-1})$. Then, m_j decreases towards zero.
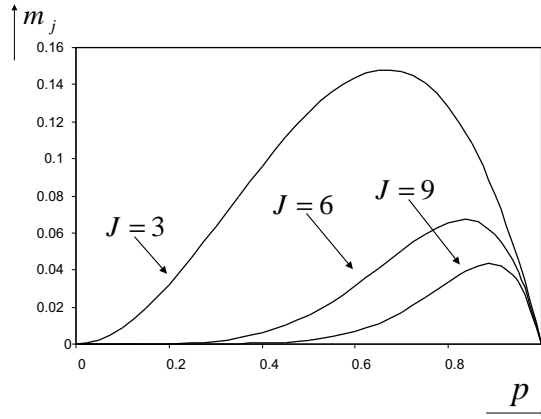

Fig. 6. m_j as a function of p for different values of $J = 3, 6, 9$ and $p' = p$.

Let m_0 be the upper bound of the probability that link (u, v) fails for the first time during one of the $f_{NDI,0}$ frames. Theorem 1, determines $f_{NDI,0}$ as function of p and m_0.

Theorem 1 *A necessary and sufficient condition for the probability that a link failure takes place for the first time in f_{NDI} frames to be smaller than or equal to m_0, is $f_{NDI} \le f_{NDI,0}$, where $f_{NDI,0} = \frac{ln(1-m_0)}{lnp}$.*

PROOF. Given that m_j is the probability that link (u, v) fails for the first time in frame j, $\sum_{j=1}^{f_{NDI}} m_j$ corresponds to the probability that link (u, v) fails

10

for the first time during one of the f_{NDI} frames. Consequently, it is required that $\sum_{j=1}^{f_{NDI}} m_j \leq m_0$, or according to Equation (5), $\sum_{j=1}^{f_{NDI}} (1-p)p^{j-1} \leq m_0$, or $(1-p)\sum_{j=1}^{f_{NDI}} p^{j-1} \leq m_0$, or $\sum_{j=1}^{f_{NDI}} p^{j-1} \leq \frac{m_0}{1-p}$. Given that $p \leq 1$, $\frac{1}{1-p} = p^0 + p^1 + p^2 + \ldots = \sum_{j=1}^{f_{NDI}} p^{j-1} + p^{f_{NDI}} + p^{f_{NDI}+1} + \ldots = \sum_{j=1}^{f_{NDI}} p^{j-1} + p^{f_{NDI}}(p^0 + p^1 + \ldots) = \sum_{j=1}^{f_{NDI}} p^{j-1} + p^{f_{NDI}} \frac{1}{1-p}$, or $\frac{1-p^{f_{NDI}}}{1-p} = \sum_{j=1}^{f_{NDI}} p^{j-1}$.

Consequently, it suffices that $\frac{1-p^{f_{NDI}}}{1-p} \leq \frac{m_0}{1-p}$, or $1 - p^{f_{NDI}} \leq m_0$, or $p^{f_{NDI}} \geq 1 - m_0$, or $f_{NDI} ln p \geq ln(1 - m_0)$, or $f_{NDI} \leq \frac{ln(1-m_0)}{ln p}$ ($ln p < 0$). Therefore, $f_{NDI,0} = \frac{ln(1-m_0)}{ln p}$. $\square$
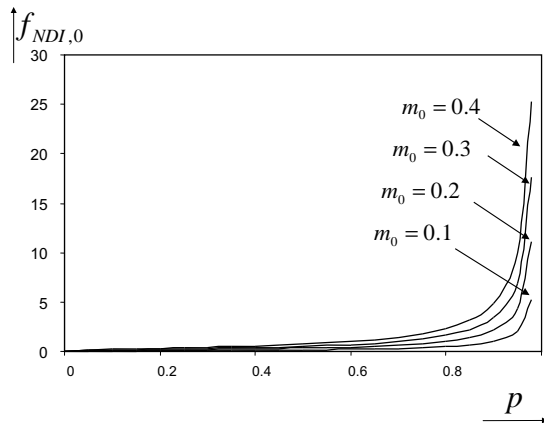

Fig. 7. $f_{NDI,0}$ as a function of p for different values of m_0 and $p' = p$.

As it may be concluded from Theorem 1, the upper bound $f_{NDI,0}$ approaches $+\infty$ for $p \to 1$ and/or $m_0 \to 1$. This is also depicted in Figure 7.

An upper bound for f_{NDI} was derived analytically such that the first link failure to be bounded by m_0. Bounding the link failure probability will decrease the wasted capacity and will likely improve the system performance, provided that sufficient traffic load is present to utilize the available capacity. The latter is taken into consideration in the next section.

5 Cluster Creation

CCR's role is to decide which nodes will create a cluster after each ND phase, depending on the topological and resource demand information, as it is described in Section 2. Specifically, a cluster will be created and will contain nodes u and v, if link (u, v) exists at frame $J = 0$ and the corresponding traffic demand λ is heavy enough (exceeding a threshold λ_0). Under such conditions, these nodes will indeed benefit from the cluster creation and the opportunity to use the higher rate second mode of operation; λ is defined to

be the (average) probability that nodes u and node v have data available for transmission between them during a frame. The objective in this section is to determine the aforementioned lower bound λ_0.

For the analysis presented in this section, it is assumed that in case of a link failure in the second mode of operation, the engaged nodes do not immediately switch to the first mode of operation. It is only after the next ND phase that they are reassigned their mode of operation, depending on the link and traffic conditions at that time. Since $\overline{J}$ is the average number of frames available for transmission during a period of F_{NDI} frames (a link is present in the second mode of operation), the average number of frames actually used for transmission (or, equivalently the average amount of data actually transmitted) is equal to $\lambda \overline{J}$. The average number of frames not used (either due to link failures or due to the absence of data traffic), denoted by L_{CCR}, is given by the following expression (by using Equation (3)),

$$L_{CCR} = f_{NDI} - \lambda f_{NDI} + \lambda(1-p)\frac{f_{NDI} + (1-p'-p)\frac{1-\left(-(1-p'-p)\right)^{f_{NDI}}}{2-p'-p}}{2-p'-p} \quad (6)$$
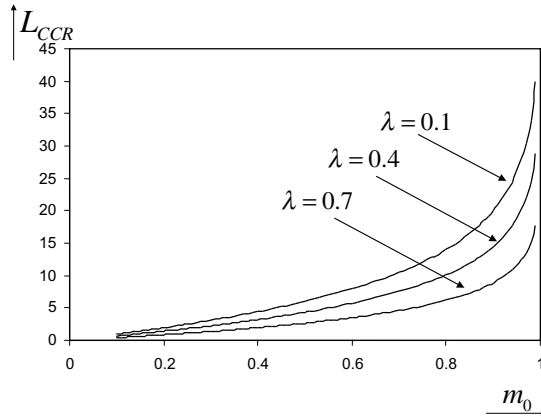

Fig. 8. L_{CCR} as a function of m_0, for different values of λ (0.1, 0.4, 0.7). $p = p' = 0.9$.

In Figure 8, L_{CCR} is depicted as a function of m_0 for different values of λ.

In order to derive a suitable lower bound for λ, it is important to exploit the potential gain of the second mode of operation due to its relatively increased data rate. Nodes that operate in the first mode of operation transmit their data according to a certain rate. Let α denote this rate, or, equivalently, the amount of data transmitted in a frame in the first mode of operation. Some nodes may select to switch to the second mode of operation is order to communicate efficiently, especially when the first mode of operation is congested due to heavy traffic load. Let β denote the rate achieved in the second mode of

12

operation, or, equivalently, the amount of data transmitted in a frame in the second mode of operation.

The system resources allocated to nodes in the second mode of operation, need to be greater than or equal to the allocated resources in the first mode of operation. Consequently, a second mode of operation should be considered if nodes are benefited from the available data rate. It is known that every $f_{ND} + f_{NDI}$ frames, a node in the second mode of operation is allowed to transmit (with rate β) for $f_{NDI} - L_{CCR}$ frames. If there was no second mode of operation available, then nodes would be allowed to transmit (with rate α) for $f_{ND} + f_{NDI}$ frames. Consequently, it should be satisfied that $\beta(f_{NDI} - L_{CCR}) \geq \alpha(f_{ND} + f_{NDI})$, or $\frac{\beta}{\alpha} \geq \frac{f_{ND} + f_{NDI}}{f_{NDI} - L_{CCR}}$. For $c = \frac{\beta}{\alpha}$, it is required that $c \geq \frac{f_{ND} + f_{NDI}}{f_{NDI} - L_{CCR}}$.

Theorem 2 *A necessary and sufficient condition for the system to be benefited by the second mode of operation, is that $\lambda \geq \lambda_0$, where $\lambda_0 = \frac{f_{NDI} + f_{ND}}{c\bar{J}}$.*

PROOF. The inequation $c(f_{NDI} - L_{CCR}) \geq f_{ND} + f_{NDI}$ may be written as $L_{CCR} \leq f_{NDI} - \frac{f_{ND} + f_{NDI}}{c}$, or $\frac{L_{CCR}}{f_{NDI}} \leq 1 - \frac{f_{ND} + f_{NDI}}{c f_{NDI}}$.

Given that $L_{CCR} = f_{NDI} - \lambda \bar{J}$, $\frac{L_{CCR}}{f_{NDI}} = 1 - \frac{\lambda \bar{J}}{f_{NDI}}$. Consequently, it suffices $\lambda \geq \lambda_0$, where $\lambda_0 = \frac{f_{NDI} + f_{ND}}{c\bar{J}}$.

It can be concluded that for $\lambda \geq \frac{f_{NDI} + f_{ND}}{c\bar{J}}$, $c \geq \frac{f_{ND} + f_{NDI}}{f_{NDI} - L_{CCR}}$, and that for $c \geq \frac{f_{ND} + f_{NDI}}{f_{NDI} - L_{CCR}}$, $\lambda \geq \frac{f_{NDI} + f_{ND}}{c\bar{J}}$.

$\square$

According to Theorem 2, if the traffic load in the network is heavy (λ close to 1), it is expected that many pairs of nodes will satisfy the condition $\lambda \geq \lambda_0$ and create clusters. Clearly, the smaller the λ_0, the larger the number of clusters created, and eventually, the larger the increment of the system performance. It is easy to conclude that small values of λ_0 are achievable for small values of f_{ND} and large values of c.

If $f_{NDI} = f_{NDI,0}$, as it is determined by Theorem 1, then λ_0 is eventually, a function of m_0 ($\bar{J}$ is a function of f_{NDI} as it can be concluded from Equation (3)). In Figure 9, λ_0 is depicted as a function of m_0, for various values of p. It can be observed that for small values of m_0, λ_0 is high. As m_0 increases, λ_0 decreases exponentially. Besides, as p increases, λ_0 decreases for the same value of m_0.

Eventually, it appears that the advantage of the second mode of operation increases as long as λ increases. Clearly, the smaller the node mobility (or, in general, the link failures) the better the overall performance. As a result, it
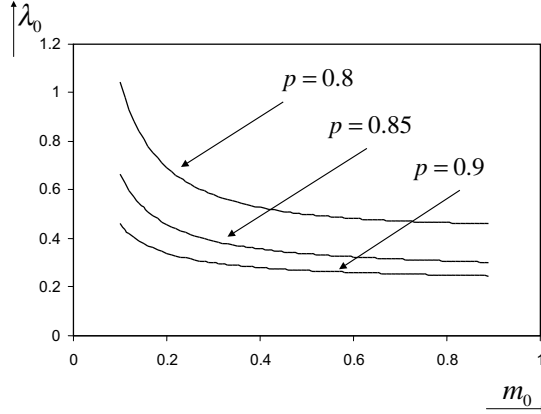
13

Fig. 9. λ_0 as a function of m_0, for different values of p. $p = p'$, $c = 5.0$, and $f_{ND} = 1.0$.

appears from the analysis that a system, based on a second mode of operation characterized by increased data rate and small range, is efficient for heavy traffic conditions and comparably small node mobility (hotspots). The following section presents simulation results that support the derived analysis.

6   Simulation Results

Simulation results are provided in this section in order to support the aforementioned analytical results. For the simulations, a network consisting of 200 nodes is implemented in a C++ environment. 100 links between those nodes are defined and a random number of them is characterized as "active" and the rest as "non-active". The links between the nodes are activated or deactivated in accordance with the 2-state Markov (Gilbert) model presented in Section 3 with corresponding probabilities p and p', respectively. Throughout the simulations, $p' = p$. The results presented in this section correspond to averaged values over 10000 runs.

It should be noted that the simulation results are very close to the theoretical ones and therefore, any observations in this section may be also made from the theoretical results presented in previous sections. However, simulation results are, most of the times, an "independent" way to confirm that the derivation of the analytical results is accurate and meaningful.

In Figure 10, p is depicted as a function of j for different values of p. The dotted lines (theoretical) depict p as it is calculated from Equation (1). The dotted lines are depicted in a continuous manner to facilitate the presentation in the figure, even though p is not a continuous function (j is an integer). As expected from the theoretical model (Equation (2)), it can be observed that for large values of j, p approaches 0.5, since $p' = p$.
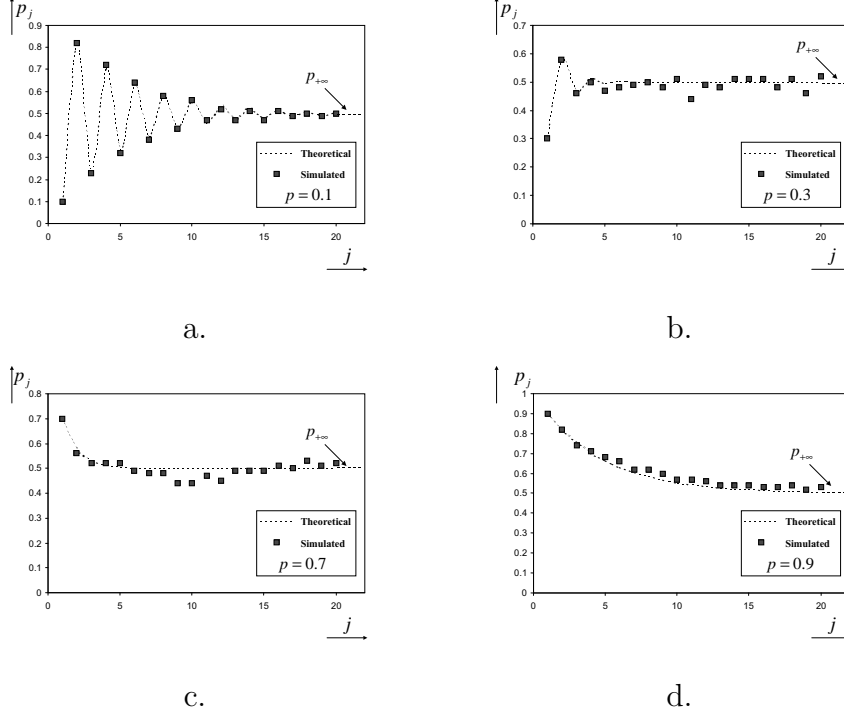
14

Fig. 10. Analytical and simulation results for p_j as a function of j for different values of p.

The depicted small squares represent the values of p_j as they were obtained using the simulator. It can be observed that these values are close to the theoretical ones.

In Figure 11, $\frac{L_{NDI}}{f_{NDI}}$ is depicted as a function of f_{NDI}. The dotted line corresponds to the curve obtained by Equation (4) and the small squares correspond to simulation results obtained for different values of f_{NDI}. It is evident that for large values of f_{NDI}, the number of lost frames (frames during which there is no connectivity between node u and node v) equals $\frac{f_{NDI}}{2}$, as expected since $p_{+\infty} = 0.5$. Consequently, a link is then expected to be available for transmission during half this number of frames.

It may be observed that for highly correlated 2-state model (e.g. $p = 0.9$) – which is the realistic case – the ratio is strictly increasing with j, and thus, the smaller the j, the higher the portion of frames to be available (the link will stay active) until the next ND phase. Simulations verify the theoretical results.

Figure 12 depicts analytical and simulation results for a number of different scenarios. It can be observed that the simulation values for m_j as a function of p, are close to the curve corresponding to the analytical results (theoretical).

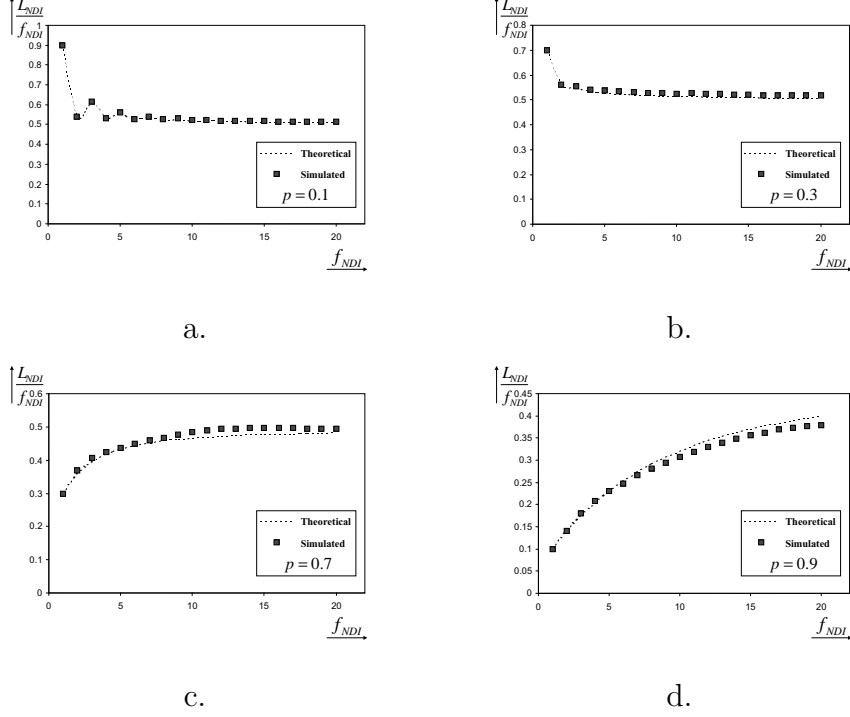In Figure 13, $f_{NDI,0}$ is depicted as a function of p. It is clear that for p close

Fig. 11. Analytical and simulation results for $\frac{L_{NDI}}{f_{NDI}}$ as a function of f_{NDI} for different values of p.
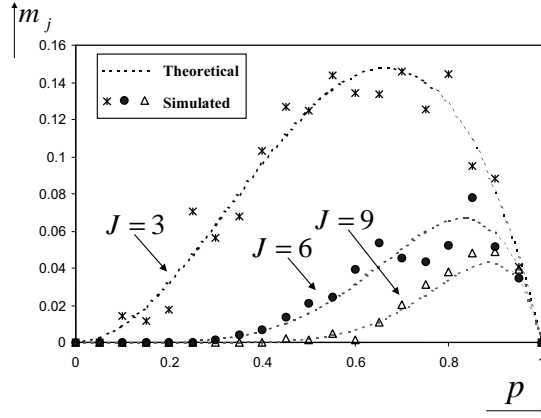

Fig. 12. Analytical and simulation results for m_j as a function of p for different values of $J = 3, 6, 9$.

to 1, $f_{NDI,0}$ approaches $+\infty$. This is expected, since for those cases that links last longer, frequent ND phases are not necessary and therefore, high values for f_{NDI} may be tolerated. Consequently, the upper bound $f_{NDI,0}$ is increased.

From Figure 14, it can be observed that L_{CCR} increases rapidly as m_0 increases. In other words, as the boundary for the probability of the first link failure in f_{NDI} frames increases (the constraint is relaxed), then the number of frames, during which link (u, v) does not exist, also increases.
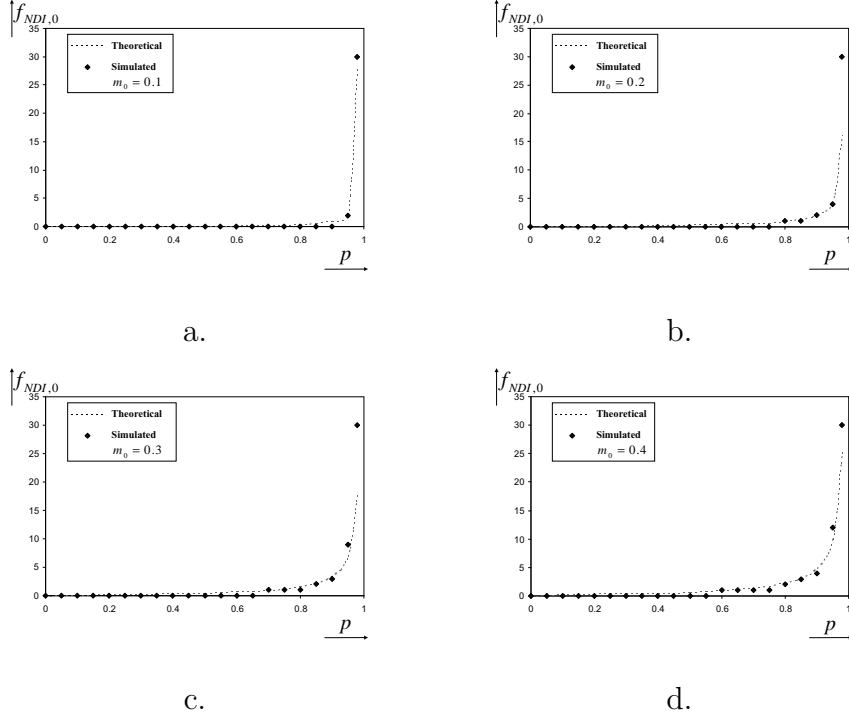
16

a.

b.

c.

d.

Fig. 13. Analytical and simulation results for $f_{NDI,0}$ as a function of p for different values of m_0.
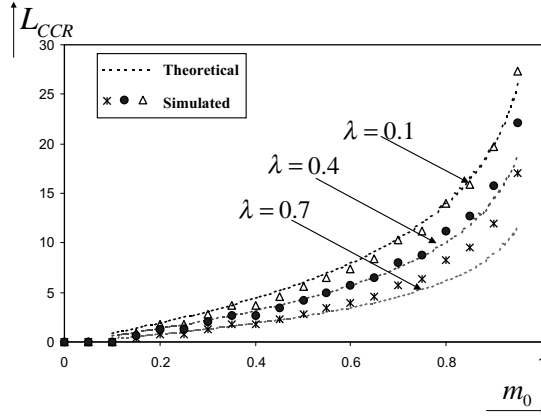

Fig. 14. Analytical and simulation results for L_{CCR} as a function of m_0, for different values of λ.

Figure 15 also presents analytical and simulation results of λ_0 as a function of m_0 for various values of p, where it can be observed that the corresponding values are close. Note that $\lambda \geq \lambda_0$ is required in order nodes to benefit from the second mode of operation. However, for small values of m_0, it may be that the number of frames, allowed for the operation at the second mode, be rather small (small values for f_{NDI}). Consequently, it may be possible that, even for $\lambda = 1$, the data exchanged during the corresponding $\overline{J}$ frames, not be enough to compensate for the frames that otherwise would have been used at
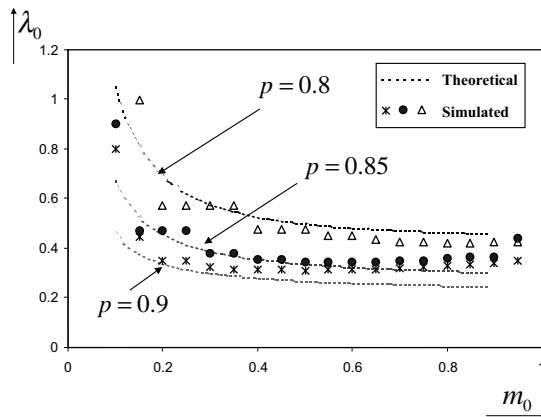
17

Fig. 15. λ_0 as a function of m_0, for different values of p. $c = 5.0$, and $f_{ND} = 1.0$.

the first mode of operation $(f_{ND} + f_{NDI})$. It may also be concluded that not only high values for λ, compared to λ_0, are desirable, but also high values for p. Consequently, the second mode of operation is beneficial for heavy traffic conditions and low node mobility.

7 Conclusions

The challenge of using a second mode of operation (WPAN) and supporting high data rates, simultaneously to the standard (first) mode of operation of a WLAN system, is analytically investigated in this work. The second mode of operation can be realized using topology control, i.e., power control, smart antennas, different frequency channels. The design requirements for the second mode of operation using different frequency channels, presented in (9), (10), are adopted and the aim is to provide analytical results showing how performance aspects of the system are affected under the induced constraints. Since supporting the second mode of operation introduces additional overhead, conditions have been established under which this overhead is compensated for and the system becomes more efficient.

A new, analytically tractable model capturing in a combined manner both the low-range communication channel behavior and the peculiar user mobility behavior in a WPAN, is proposed and constructed. A number of analytical results are obtained by incorporating this model in a WLAN/WPAN environment. In particular, an upper bound $(f_{NDI,0})$ regarding the number of frames between consecutive ND phases, is analytically determined, with respect to the probability of the first link failure. Given that frequent ND phases allow for an increased overhead, it is obvious that this upper bound is essential for the overall system performance. Since nodes in proximity to each other may not have large amounts of data to exchange, a lower bound of the traffic load

18

(λ_0) among two nodes, is also analytically determined to allow for a more efficient use of the second mode of operation. If the condition $\lambda \geq \lambda_0$ is satisfied, the second mode of operation may be employed efficiently. Simulation results support the claims and the expectations of the aforementioned analysis.

In conclusion, the lower the node mobility in a WPAN environment and the higher the traffic load among nodes, the higher the achievable user rates. The results of the analytical study, supported also by the simulation results, prove not only the aforementioned statement but also provide for exact boundaries regarding system performance improvement when taking advantage of a dual-mode system.

8 Acknowledgement

A Markov State Diagram Analysis

Let

$$\mathbf{P}^{(j)} = \left[p_j \ p_j' \right].$$

Given that for $J = 0$, $p_0 = 1$ and $p_0' = 0$. Consequently,

$$\mathbf{P}^{(j)} = \left[1 \ 0 \right] \begin{bmatrix} p & 1-p \\ 1-p' & p' \end{bmatrix}^{(j)}.$$

From the previous equation, it can be calculated that $p_{j+1} = pp_j + (1 - p')p_j'$. Given that $p_j = 1 - p_j'$, the previous equation may be written as $p_{j+1} = pp_j + (1 - p')(1 - p_j)$, or $p_{j+1} = pp_j + (1 - p') - (1 - p')p_j$, or $p_{j+1} = (1 - p') - (1 - p' - p)p_j$, where $p_0 = 1$. It is also satisfied that $p_j = (1 - p') - (1 - p' - p)p_{j-1}$. Consequently, $p_{j+1} - p_j = -(1 - p' - p)p_j + (1 - p' - p)p_{j-1} = -(1 - p' - p)(p_j - p_{j-1})$.

For simplicity, let $X = -(1-p'-p)$ and $K_j = p_j - p_{j-1}$. Clearly, $K_j = XK_{j-1}$, where $K_1 = p_1 - p_0 = (1-p') - (1-p'-p)p_0 - 1 = p - 1$. Consequently, $K_2 = XK_1 = X(p-1)$, $K_3 = XK_2 = X^2(p-1)$, ..., $K_j = XK_{j-1} = X^{j-1}(p-1)$. Given that, $K_1 = p_1 - p_0$, $K_2 = p_2 - p_1$, ..., $K_j = p_j - p_{j-1}$, after the summation of the left hand parts of the previous equations, $\sum_{i=1}^{j} K_i = p_j - p_0 = p_j - 1$, or $\sum_{i=1}^{j} X^{i-1}(p-1) = p_j - 1$, or $p_j = 1 - (1-p)\sum_{i=1}^{j}(-(1-p'-p))^{i-1}$.

It is known that for $|y| < 1$, $\frac{1}{1+y} = y^0 - y^1 + y^2 - y^3 \dots$ Suppose that j is an even number and $y = 1 - p' - p$. It is satisfied that $\frac{1}{1+y} = y^0 - y^1 + y^2 - y^3 \dots + y^{j-2} - y^{j-1} + y^j - y^{j+1} \dots$, or $\frac{1}{1+y} = \sum_{i=1}^{j} y^{i-1} + y^j - y^{j+1} \dots$, or $\frac{1}{1+y} = \sum_{i=1}^{j} y^{i-1} + y^j(y^0 - y^1 + y^2 - y^3 \dots)$, or $\frac{1}{1+y} = \sum_{i=1}^{j} y^{i-1} + y^j \frac{1}{1+y}$. Finally, $\sum_{i=1}^{j} y^{i-1} = \frac{1-y^j}{1+y}$, provided that j is an even number. For the case that j is an odd number, it can be shown that $\sum_{i=1}^{j} y^{i-1} = \frac{1+y^j}{1+y}$. Therefore, for all j, $\sum_{i=1}^{j} y^{i-1} = \frac{1-(-y)^j}{1+y}$. Consequently, $p_j = 1 - (1-p)\frac{1-\left(-(1-p'-p)\right)^j}{2-p'-p}$.

When $j \to +\infty$,

$$\begin{bmatrix} p_{+\infty} & 1 - p_{+\infty} \end{bmatrix} \begin{bmatrix} p & 1-p \\ 1-p' & p' \end{bmatrix} = \begin{bmatrix} p_{+\infty} \\ 1 - p_{+\infty} \end{bmatrix}.$$

It can be calculated that $p_{+\infty} = \frac{1-p'}{2-p-p'}$.

B Derivation of Equation (3)

According to Equation (1), $p_j = 1 - (1-p)\frac{1-\left(-(1-p'-p)\right)^j}{2-p'-p}$. Consequently, $\overline{J} = \sum_{j=1}^{f_{NDI}} p_j = \sum_{j=1}^{f_{NDI}} \left(1 - (1-p)\frac{1-\left(-(1-p'-p)\right)^j}{2-p'-p}\right) = f_{NDI} - (1-p)\frac{f_{NDI} - \sum_{j=1}^{f_{NDI}}\left(-(1-p'-p)\right)^j}{2-p'-p}$.

It is known that $\frac{1}{1+x} = x^0 - x^1 + x^2 - x^3 \dots$ Let $x = 1 - p' - p$. If f_{NDI} is an even number, $\sum_{j=1}^{f_{NDI}}(-x)^j = -x^1 + x^2 - x^3 \dots - x^{f_{NDI}-1} + x^{f_{NDI}} = -x\left(x^0 - x^1 + x^2 \dots + x^{f_{NDI}-2} - x^{f_{NDI}-1}\right)$. It is known that, $\frac{1}{1+x} = x^0 - x^1 + x^2 \dots + x^{f_{NDI}-2} - x^{f_{NDI}-1} + x^{f_{NDI}} - x^{f_{NDI}+1} \dots = x^0 - x^1 + x^2 \dots + x^{f_{NDI}-2} - x^{f_{NDI}-1} + x^{f_{NDI}}\left(x^0 - x^1 + x^2 \dots\right) = x^0 - x^1 + x^2 \dots + x^{f_{NDI}-2} - x^{f_{NDI}-1} + \frac{x^{f_{NDI}}}{1+x}$ or, $\frac{1-x^{f_{NDI}}}{1+x} = x^0 - x^1 + x^2 \dots + x^{f_{NDI}-2} - x^{f_{NDI}-1}$. Consequently, $\sum_{j=1}^{f_{NDI}}(-x)^j = -x\frac{1-x^{f_{NDI}}}{1+x}$, provided that j is an even number. If j is an odd number it may be calculated that $\sum_{j=1}^{f_{NDI}}(-x)^j = -x\frac{1+x^{f_{NDI}}}{1+x}$. Finally, for all j, $\sum_{j=1}^{f_{NDI}}(-x)^j = -x\frac{1-(-x)^{f_{NDI}}}{1+x}$. ¿From the previous it may be easily calculated that $\overline{J} = f_{NDI} -$

$$(1-p)^{\frac{f_{NDI}+(1-p'-p)\frac{1-\left(-(1-p'-p)\right)^{f_{NDI}}}{2-p'-p}}{2-p'-p}}.$$

C   Summary of Parameters

Parameter	Description
f_{ND}	Number of frames required for a ND phase
f_{NDI}	Number of frames between two consecutive ND phases
(u,v)	Link between node u and node v
j	Number of frames after the creation of a cluster
J	Random variable that takes values j
p_j	Probability that link (u,v) exists in frame $J=j$ provided that it existed at the ND phase
p	Probability that link (u,v) exists in frame $J=j$, provided that it existed in frame $J=j-1$
p'	Probability that link (u,v) does not exist in frame $J=j$, provided that it did not exist in frame $J=j-1$
$\overline{J}$	Average number of frames that link (u,v) exists in a cluster
L_{NDI}	Number of number of frames not used due to lost connectivity
m_j	Probability the link (u,v) first fails at frame $J=j$
m_0	Upper bound of the probability m_j for any frame $J=j$
$f_{NDI,0}$	Upper bound of f_{NDI}
λ	Probability that nodes u and v want to exchange data in a frame over link (u,v) and no other link
λ_0	Lower bound of the value of $\lambda_{(u,v)}$
L_{CCR}	Number of frames not used due to lost connectivity or absence of data transmission
α	The average data rate at the first mode of operation
β	The average data rate at the second mode of operation
c	Ratio of β over α

References

[1] K. Ahmavaara, H. Haverinen, R. Pichna, "Interworking Architecture between 3GPP and WLAN Systems," IEEE Communications Magazine, vol.41, no.11, Nov. 2003, pp.74-81.

[2] A. Salkintzis, "Interworking Techniques and Architectures for WLANs/3G Integration toward 4G Mobile Data Networks," IEEE Wireless Communications, vol. 11, no.3, June 2004.

[3] H. Y. Hsieh and R. Sivakumar, "On Using the Ad-Hoc Network Model in Cellular Packet Data Networks," in Proc. ACM MOBIHOC 2002, Lausanne, Switzerland, June 2002.

[4] Y. D. Lin and Y. C. Hsu, "Multi-hop Cellular: A New Architecture for Wireless Communications," in Proc. IEEE INFOCOM 2000, Tel Aviv, Israel, March 2000.

[5] A. Panagakis, E. Balafoutis and I. Stavrakakis, "Study of the Capacity of Multi-hop Cellular Networks," in Proc. Quality of Future Internet Services (QoFIS) 2003, Stockholm, Sweden, October 2003.

[6] H. Y. Hsieh and R. Sivakumar, "Performance Comparison of Cellular and Multi-hop Wireless Networks: A Quantitative Study," in Proc. ACM SIGMETRICS 2001, Cambridge, MA, USA, June 2001.

[7] K. Jayanth Kumar, B. S. Manoj, C. Siva Ram Murthy, "MuPAC: Multi-power Architecture for Cellular Networks," in Proc. IEEE PIMRC 2002, Lisbon, Portugal, September 2002.

[8] M. Lott, M. Weckerle, W. Zirwas, H. Li, E. Schulz, "Hierarchical Cellular Multihop Networks," in Proc. EPMCC 2003, Glascow, Scotland, April 2003.

[9] K. Oikonomou, A. Vaios, S. Simoens, P. Pellati, I. Stavrakakis, "A Centralized Ad-Hoc Network Architecture (CANA) Based on Enhanced HiperLAN/2," in Proc. IEEE PIMRC 2003, Beijing, China, September 2003.

[10] A. Vaios, K. Oikonomou, N. Zinelis, I. Stavrakakis, "Increasing Capacity in Dual-Band WLANs through Ad-hoc Networking," International Journal of Wireless and Mobile Computing (IJWMC), Special Issue on Wireless Ad Hoc Networking (to appear in 2005).

[11] K. Oikonomou, N. Pronios, I. Stavrakakis, "Performance Analysis of TDMA MAC Schemes for Ad-Hoc Networks with Topology Control," The Third Annual Mediterranean Ad Hoc Networking Workshop (Med-Hoc-Net 2004), Bodrum, Turkey, June 2004.

[12] N. Pronios, "Performance Considerations for Slotted Spread-spectrum Random Access Networks with Directional Antennas," in Proc. IEEE GLOBECOM '89, November 1989.

[13] Y.B. Ko, V. Shankarkumar, N.H. Vaidya, "Medium Access Control Protocols Using Directional Antennas in Ad-hoc Networks," in Proc. INFOCOM 2000, Tel Aviv, Israel, March 2000.

[14] J. Ward and R. T. Compton, "Improving the Performance of Slotted

ALOHA Packet Radio Network with an Adaptive Array," IEEE Transactions on Communications, 40(2):292–300, February 1992.

[15] R. T. Compton and J. Ward, "High Throughput Slotted ALOHA Packet Radio Networks with Adaptive Arrays," IEEE Transactions on Communications, vol. 41, no. 3, pp. 460-470, March 1993.

[16] R. Wattenhofer, L. Li, P. Bahl, Y. M. Wang, "Distributed Topology Control for Power Efficient Operation in Multihop Wireless Ad-hoc Networks," in Proc. IEEE INFOCOM 2001, Anchorage, Alaska, April 2001.

[17] M. Kubisch, H. Karl, A. Wolisz, L. C. Zhong, J. Rabaey, "Distributed Algorithms for Transmission Power Control in Wireless Sensor Networks," in WCNC 2003, New Orleans, LA, March 2003.

[18] J. Monks, V. Bharghavan, W. W. Hwu, "Transmission Power Control for Multiple Access Wireless Packet Networks," in Proc. IEEE LCN 2000, Tampa, FL, November 2000.

[19] S. Narayanaswamy, V. Kawadia, R. S. Sreenivas, P. R. Kumar, "Power Control in Ad-hoc Networks: Theory, Architecture, Algorithm and Implementation of the COMPOW protocol," in Proc. of European Wireless Conference, 2002.

[20] J. P. Monks, J.-P. Ebert, A. Wolisz, Wen-mei W. Hwu, "A Study of the Energy Saving and Capacity Improvement Potential of Power Control in Multi-hop Wireless Networks," in Workshop on Wireless Local Networks, Tampa, Florida, USA, also Conf. of Local Computer Networks (LCN), November 2001.

[21] M. Johnson, "HiperLAN/2 - The Broadband Radio Transmission Technology Operating in the 5 GHz Frequency Band," available via the HiperLAN/2 Global Forum, *http://www.hiperlan2.com.*

[22] T. Chu and I. Nikolaidis, "On the artifacts of random waypoint simulations," in Proc. of the 1st International Workshop on Wired/Wireless Internet Communications (WWIC2002) in conjunctions with the International Conference on Internet Computing (IC'02), 2002.